Volume 1 | Number 1 | Jan 2013 | Pages 1–100

## ChemComm

Chemical Communications
www.rsc.org/chemcomm

ROYAL SOCIETY OF CHEMISTRY

ROYAL SOCIETY OF CHEMISTRY

www.rsc.org/chemcomm

# Journal Name

## COMMUNICATION

# Chiral All-Organic Nitroxide Biradical Liquid Crystal Showing Remarkably Large Positive Magneto-LC Effects

Katsuaki Suzuki,[a] Yusa Takemoto,[a] Shohei Takaoka,[a] Koji Taguchi,[a] Yoshiaki Uchida,[b,c] Dmitrii G. Mazhukin,[d,e] Igor A. Grigor'ev[d] and Rui Tamura*[a]

**The liquid crystalline chiral nitroxide biradical (*S,S,S,S*)-3 synthesized has shown much larger 'positive magneto-LC effects' in the chiral nematic (N\*) phase than in that of the monoradical (*S,S*)-1.**

Magnetic liquid crystals (LCs) have attracted great concern as soft materials to enhance the effect of magnetic fields on the electric and optical properties of LCs.[1] For example, they were anticipated to exhibit unique magnetic interactions and thereby unconventional magneto-electric or magneto-optical coupling[2,3] in the liquid crystalline (LC) state under external magnetic fields. However, there had been no prominent study on this interesting topic before 2004, because the majority of magnetic LCs were highly viscous transition or lanthanide metal-containing LCs which were not always appropriate for investigating the swift molecular motion and reorientation in the LC phases in low applied magnetic fields due to the high viscosity.[1] Recently it has been revealed that bent-core mesogens containing 6-oxoverdazyl radical as the angular central unit exhibit photoinduced ambipolar charge transport and electrooptical effects in the tetragonal phase.[4] However, they showed a paramagnetic behaviour in the isotropic phase and a gradual increase of antiferromagnetic interactions in the LC phase upon cooling.

In this context, in 2008 we reported that chiral all-organic rod-like LC compounds **1** with a stable nitroxide radical unit in the central core position and a negative dielectric anisotropy ($\Delta\varepsilon < 0$) (Fig. 1)[5] exhibited a sort of spin glass-like inhomogeneous ferromagnetic interactions (the average spin-spin exchange interaction constant $\bar{J} > 0$) induced by application of low magnetic fields in the LC phases at high temperatures (30–150 °C).[6,7] By electron paramagnetic resonance (EPR) spectroscopic studies and DFT calculations, such a unique magnetic phenomenon, which was referred to as 'positive magneto-LC effects',[8] was correlated with the preferential occurrence of ferromagnetic spin-spin dipole interactions in magnetic fields due to the inhomogeneous intermolecular contacts in the LC phases.[9,10] Furthermore, interestingly, larger positive magneto-LC effects were revealed to occur in the chiral LC phases than in the corresponding achiral ones.[6-9] Thus far, it is not clear why such large ferromagnetic interactions were observed in these LC phases, particularly in chiral ones, at high temperatures.

Meanwhile, as another example, in 2014 an achiral hexa-peri-hexabenzocoronene derivative carrying a conjugated *tert*-butyl nitroxide moiety has been reported to show the positive magneto-LC effects in the columnar hexagonal LC phase,[11] although all of other three achiral all-organic radical columnar discotic LC compounds reported before 2014 did not show the positive magneto-LC effects.[12-14]

Here we report the preparation of (*S,S,S,S*)-**3** as the first all-organic biradical LC compound which showed remarkably large magneto-LC effects in the chiral nematic (N\*) phase. The biradical compound (*S,S,S,S*)-**3** (>99% *ee*, Fig. S1 and S2, ESI) was prepared by condensation of *p*-hydroxybenzyl alcohol and two equiv of the benzoic acid derivative (*S,S*)-**2** containing a cyclic nitroxide radical group on the para position using 1-ethyl-3-(3-dimethylaminopropyl)carbodiimide hydrochloride (EDC) and a catalytic amount of 4-dimethylaminopyridine (DMAP) in dichloromethane (Fig. 1 and for the details, ESI).

[a.] Graduate School of Human and Environmental Studies, Kyoto University, Kyoto 606-8501, Japan. E-mail: tamura.rui.8c@kyoto-u.ac.jp; Fax: +81-75-753-7915
[b.] Graduate School of Engineering Science, Osaka University, Toyonaka, Osaka 560-8531, Japan
[c.] . Japan Science and Technology Agency, PRESTO, 4-1-8 Honcho, Kawaguchi, Saitama 332-0012, Japan
[d.] N. N. Vorozhtsov Novosibirsk Institute of Organic Chemistry, Siberian Branch of Russian Academy of Sciences, 9 Akademika Lavrentieva Ave., Novosibirsk 630090, Russia
[e.] Novosibirsk State University, 2 Pirogova St., Novosibirsk 630090, Russia
†Electronic Supplementary Information (ESI) available: [Synthesis, HPLC chromatograms, XRD patterns, $\chi_M$–$T$ plots and selected EPR spectra of (*S,S,S,S*)-**3**; derivation of relative paramagnetic susceptibility ($\chi_{rel}$) from EPR spectra]. See DOI: 10.1039/x0xx00000x
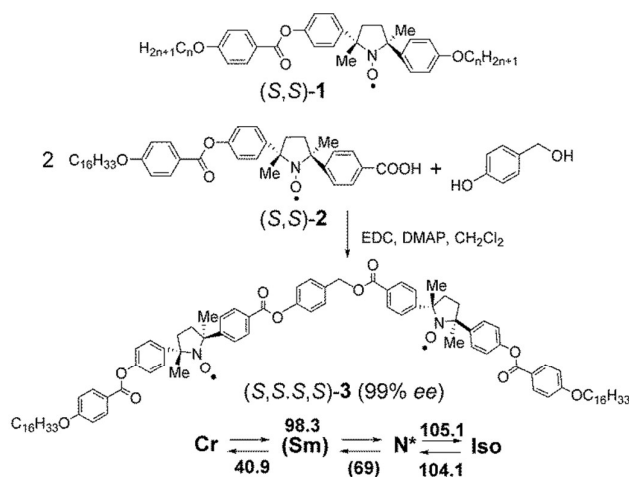
**Fig. 1** Molecular structure of monoradical compounds (*S,S*)-**1** and preparation of biradical compound (*S,S,S,S*)-**3** from (*S,S*)-**2**. The phase transition temperatures of (*S,S,S,S*)-**3** were determined by DSC analysis and POM observation.

The phase transition behavior of (*S,S,S,S*)-**3** was characterized by differential scanning calorimetry (DSC) (Fig. 2a), polarized optical microscopy (POM) (Fig. 2b-d), and X-ray diffraction (XRD) analysis (Fig S3, ESI). (*S,S,S,S*)-**3** showed an enantiotropic N* phase and a monotropic smectic (Sm) phase. The fan-like and fingerprint textures characteristic of an N* phase were observed in the 1st cooling and 2nd heating runs, respectively (Fig. 2b and d).[15] The metastable Sm phase was detected only at a scanning rate of more than 10 °C min$^{-1}$ in the cooling run; the pseudo-isotropic texture (Fig. 2c) and sharp low angle XRD peak at 2.15° (Fig. S3c, ESI) were observed in the cooling run. The observed N* phase may contain smectic cybotactic groups,[16] because the enthalpy (Δ*H*) at the N*-to-Sm transition was negligible (Fig. 2a) and the small XRD peak at 5.7° may correspond to smectic fluctuations. In this study, we have focused on the change in magnetic properties at the crystal-to-N* phase transition of (*S,S,S,S*)-**3**, since the metastable Sm phase was not suited for the time-consuming measurement of magnetic properties by VT-EPR spectroscopy.
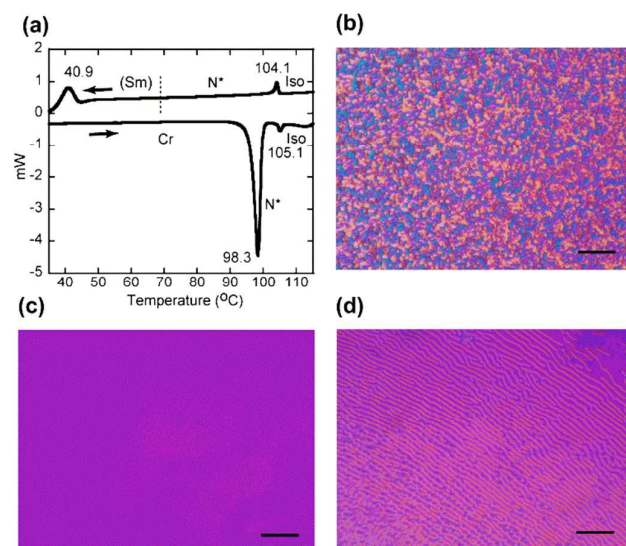


**Fig. 2** Phase transition behavior of (*S,S,S,S*)-**3**. (a) DSC curves at a scanning rate of 10 °C min$^{-1}$ in the first heating and cooling runs. The dotted line represents the N*-to-Sm phase transition temperature determined by POM observation. The enthalpies Δ*H*'s (kJ mol$^{-1}$) were 28.6 and 1.9 at 98.3 °C and 105.1 °C, respectively, in the heating run, and 3.6 at 104.1 °C in the cooling run. Polarized optical microphotographs were taken under random conditions in the cooling run: (b) the fan-like texture for the short pitch N* phase at 80 °C in the first cooling run, (c) the pseudo-isotropic texture for the Sm phase at 65 °C in the first cooling run and (d) the fingerprint texture for the N* phase at 100 °C in the second heating run from the Sm phase. The scale bar at the lower right in each photograph corresponds to 100 μm.

To confirm whether the stable N* phase of (*S,S,S,S*)-**3** shows the positive magneto-LC effects, the temperature dependence of molar magnetic susceptibility ($\chi_M$) was measured at a magnetic field of 0.05 T on a SQUID magnetometer using a paramagnetic aluminum pan to minimize the experimental error at high temperatures (Fig. 3).[7,8] Here $\chi_M$ is used as the sum of paramagnetic susceptibility ($\chi_{para}$) and diamagnetic susceptibility ($\chi_{dia}$), as we cannot exactly determine the $\chi_{para}$ in the magnetic LC phases due to the temperature-dependent nature of the $\chi_{dia}$ in LC phases.[17] With respect to the crystalline phase, the obtained $\chi_{para}T$–$T$ plots obeyed the Curie-Weiss law in the temperature range between 100 and 300 K [$\chi_M = C/(T - \theta) + \chi_{dia}$: Weiss constant $\theta = -3.0$ K, Curie constant $C = 0.75$ emu K mol$^{-1}$ and $\chi_{dia} = -8.50$ x $10^{-4}$ emu mol$^{-1}$] (Fig. S4, ESI), exhibiting neither appreciable intramolecular nor intermolecular magnetic interactions in this temperature interval and no contamination of paramagnetic impurities. In fact, the distance between two nitroxide radicals calculated from the optimized molecular structure of **3** obtained by the Density Functional Theory calculation (Gaussian 09)[18] was ca. 19 Å (Fig. 4), which was too long to produce appreciable spin-spin exchange interactions between two paramagnetic centers in the molecule. Actually, EPR spectra characteristic of independent two nitroxide radicals in a molecule were observed in the diluted THF solution (5 x 10$^{-4}$ mol L$^{-1}$) of (*S,S,S,S*)-**3** at 25 °C and at –150 °C (Fig. S5, ESI). These results clearly demonstrate the absence of intramolecular exchange interactions.
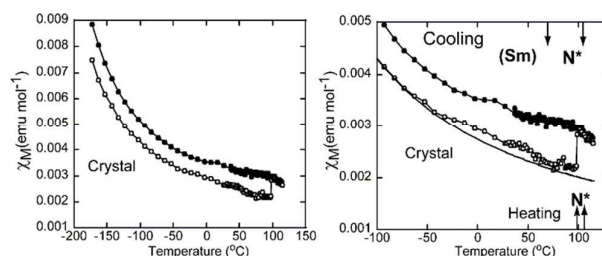


**Fig. 3** Temperature dependence of molar magnetic susceptibility ($\chi_M$) of (*S,S,S,S*)-**3** at a field of 0.05 T in the temperature range of (a) –170 to +120 °C and (b) –100 to +120 °C (magnification) measured by using a paramagnetic aluminium pan. Open and filled circles represent the first heating and cooling runs, respectively. The solid line shows the Curie-Weiss fitting curve. The LC phase transition temperatures, which were determined by DSC analysis at a scanning rate of 10 °C min$^{-1}$ and POM observation in the heating and cooling runs, are indicated by arrows in the lower and upper sides in panel b, respectively.

Interestingly, a considerable $\chi_M$ increase of as large as 38% was noted for (*S,S,S,S*)-**3** at the crystal-to-N* phase transition (98°C) in the heating run (Fig. 3 and Fig. S6, ESI). This $\chi_M$ increase is much larger than that (30%) of (*S,S*)-**1** (n = 8).[7] However, the scatter of the $\chi_M$–*T* plots for (*S,S,S,S*)-**3** at higher temperatures was too large to

discuss the details of the temperature dependence of the magnetic interactions. Therefore, we evaluated the paramagnetic susceptibility by VT-EPR spectroscopy using a quartz sample tube (Fig. S7 ESI), which allows us to ignore the $\chi_{dia}$ term and to understand the magnetic interactions in-depth.[7,8]

The temperature dependence of the paramagnetic susceptibility indicated in relative units ($\chi_{rel}$) for (*S,S,S,S*)-**3** is shown in Fig. 5a. In the heating run, the $\chi_{rel}$ abruptly increased at the crystal-to-N* transition. In the cooling run, $\chi_{rel}$ increased with decreasing temperature in the isotropic and N* phases and abruptly decreased at the N*-to-crystal phase transition (at 66 °C), indicating the disappearance of the metastable Sm phase owing to the very slow cooling rate in the quartz tube. The difference in the $\chi_{rel}$ value between the crystalline phases before the heating run and immediately after the cooling run was ascribed to polymorphism (Fig. S3a and S3d, ESI). Thus, we could indicate that the behavior of paramagnetic susceptibility found by EPR spectroscopy correlates with that of the molar magnetic susceptibility determined by SQUID measurement.
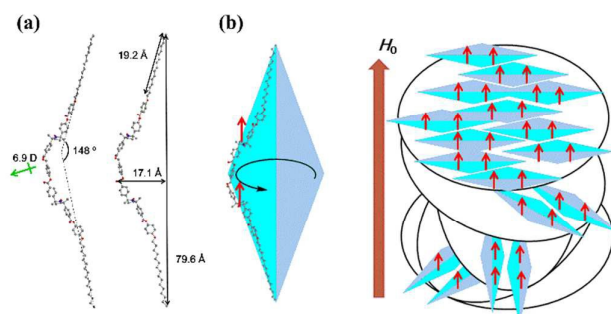


**Fig. 4** Molecular structure of (*S,S,S,S*)-**3** and LC superstructure in the N* phase. (a) The molecular conformation optimized by the Monte Carlo method using the Merck Molecular Force Field (MMFF), followed by Density Functional Theory calculation at the UB3LYP/6-31G(d) level (Gaussian 09). The unit of distance is Å. (b) Schematic illustration of assumed magnetic interactions in the N* phase
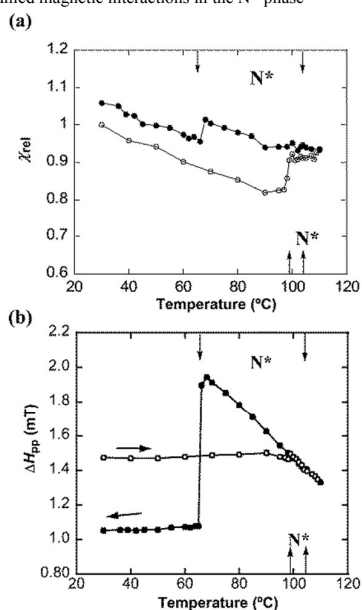


**Fig. 5** Temperature dependence of (a) $\chi_{rel}$ and (b) $\Delta H_{pp}$ for (*S,S,S,S*)-**3** by EPR spectroscopy around a field of 0.33 T. The $\chi_{rel}$ is the relative paramagnetic susceptibility, which is defined as $\chi_{para}/\chi_0$, where $\chi_0$ is the paramagnetic susceptibility at 30 °C in the heating run. The spectra which were measured five times at each temperature were accumulated. The EPR signal intensity obtained by numerical double integration of each spectrum was used as the $\chi_{para}$. Open and filled circles represent the first heating and cooling runs, respectively. The LC phase transition temperatures determined by DSC analysis at a scanning rate of 10 °C min$^{-1}$ in the heating and cooling runs are shown by arrows in the lower and upper parts in each panel, respectively.

To gain an insight into the origin of positive magneto-LC effects ($\bar{J} > 0$) operating in the N* phase of (*S,S,S,S*)-**3**, the temperature dependence of EPR peak-to-peak line width ($\Delta H_{pp}$) was compared with that of the $\chi_{rel}$ (Fig. 5b). Generally, the change in $\Delta H_{pp}$ reflects the following two magnetic interactions: (a) spin-spin dipole interaction (the stronger the interaction, the more the $\Delta H_{pp}$ increase) and (b) spin-spin exchange interaction (the stronger the interaction, the more the $\Delta H_{pp}$ decrease). In the present case, a slight increase in $\Delta H_{pp}$ occurred in concert with the abrupt increase in $\chi_M$ at the crystal-to-N* transition (98 °C) in the heating run, indicating the increase of spin-spin dipole interactions in the N* phase. These results support that strong intermolecular spin-spin dipole as well as exchange interactions must operate by introducing independent two nitroxide radical units in a molecule (Fig. 4b).

To visualize the large positive magneto-LC effects of (*S,S,S,S*)-**3**, the N* droplet with a diameter of approximately 2 mm was prepared by floating the melted LC compound on hot water at 75°C by using a small plastic spatula and then a rod-like permanent magnet (maximum 0.5 T, 6 mm φ x 20 mm) approached. Consequently, the N* droplet of (*S,S,S,S*)-**3** responded to the action of the magnet much more quickly (Movie S1, ESI) than that of (*S,S*)-**1** (n = 8).[7] This result indicates that the difference in the response to the magnet between the two N* droplets of (*S,S,S,S*)-**3** and (*S,S*)-**1** (n = 8) should depend not only on the interfacial interaction between the N* droplet and water but also on the magnitude of positive magneto-LC effects.

We described the preparation and outstanding magnetic properties of the chiral all-organic nitroxide biradical (*S,S,S,S*)-**3** showing a stable N* phase. The hitherto largest positive magneto-LC effects (38% $\chi_M$ increase) were observed in the biradical N* phase. The VT-EPR spectroscopic analysis supports that the occurrence of such large positive magneto-LC effects originates from increased intermolecular spin-spin exchange and dipole interactions due to inhomogeneous intermolecular short contacts in the biradical N* phase.[9,10] These results imply that if a chiral bent-core ferroelectric[19] biradical compound with large positive magneto-LC effects is available it is expected to show a larger magneto-electric coupling[2] than the rod-like ferroelectric monoradical (*S,S*)-**1** (n = 13) exhibited at high temperatures.[20] Furthermore, these results would provide useful information to prepare metal-free magnetic soft nanomaterials, such as magneto-active nanoemulsions and nanotubes, which are expected to be used for biomedical applications including the oxidation & reduction-resistant,[21] magnetic resonance imaging (MRI) contrast agents and the magnetic carrier for a magnetically targeted drug-delivery system in place of magnetoliposomes containing $Fe_3O_4$,[22] because stable nitroxide radicals are known to be nontoxic to cell and animals.[23]

## Notes and references

1 L. M. Blinov, *Electro-Optical and Magneto-Optical Properties of Liquid Crystals*, John Wiley & Sons, New York, 1983; J.-L. Serrano, *Metallomesogens: Synthesis, Properties, and Applications*. Wiley-VCH, Weinheim, 1996; D. Dunmur, K. Toriyama, *Physical Properties of Liquid Crystals*, eds. D. Demus, J. Goodby, G. W. Gray, H. W. Spiess, V. Vill, Wiley-VCH, Weinheim, 1999, pp. 102-112; P. Kaszynski, *Magnetic Properties of Organic Materials*, ed. P. M. Lahti, Marcel Dekker, New York, 1999, pp. 305-324; K. Griesar, W. Haase, *Magnetic Properties of Organic Materials*, ed. P. M. Lahti, Marcel Dekker, New York, 1999, pp. 325-344; K. Binnemans, C. Gröller-Walrand, *Chem. Rev.*, 2002, **102**, 2303.

2 W. Eerenstein, N. D. Mathur, J. F. Scott, *Nature*, 2006, **442**, 759; C. N. R. Rao, C. R. Serrao, *J. Mater. Chem.*, 2007, **17**, 4931; C. Felser, G. H. Fecher, B. Balke, *Angew. Chem. Int. Ed.*, 2007, **46**, 668; S. Seki, *Magnetoelectric Response in Low-Dimensional Frustrated Spin Systems*, Springer, Tokyo, 2012.

3 G. L. J. A. Rikken, E. Raupach, *Nature*, 1997, **390**, 493; G. L. J. A. Rikken, E. Raupach, *Nature*, 2000, **405**, 932; C. Train, R. Gheorghe, V. Krstic, L. M. Chamoreau, N. S. Ovanesyan, G. L. J. A. Rikken, M. Gruselle, M. Verdaguer, *Nature Mater.*, 2008, **7**, 729.

4 M. Jasiński,, D. Pociecha, H. Monobe, J. Szczytko, P. Kaszyński, *J. Am. Chem. Soc.*, 2014, **136**, 14658-14661.

5 N. Ikuma, R. Tamura, S. Shimono, N. Kawame, O. Tamada, N. Sakai, J. Yamauchi, Y. Yamamoto, *Angew. Chem. Int. Ed.*, 2004, **43**, 3677; N. Ikuma, R. Tamura, S. Shimono, Y. Uchida, K. Masaki, J. Yamauchi, Y. Aoki, H. Nohira, *Adv. Mater.*, 2006, **8**, 477.

6 Reviews: R. Tamura, Y. Uchida, N. Ikuma, *J. Mater. Chem.*, 2008, **18**, 2872; G. I. Likhtenshtein, J. Yamauchi, S. Nakatsuji, A. I. Smirnov, R. Tamura, *Nitroxides: Application in Chemistry, Biomedicine, and Materials Science*, Wiley-VCH, Weinheim, **2008**, pp. 303- 329; R. Tamura, N. Ikuma, S. Shimono, *Soft Nanomaterials*. *Vol.* 1, ed. H. S. Nalwa, American Scientific Publishers, CA, 2009, pp. 257-277; R. Tamura, Y. Uchida, K. Suzuki, K. *Liquid Crystals Beyond Display: Chemistry, Physics, and Applications*, ed. Q. Li, John Wiley & Sons, Hoboken, 2012, pp. 83-110; R. Tamura, Y. Uchida, K. Suzuki, *Nitroxides: Theory, Experiment and Applications*, ed. A. I. Kokorin, InTech, Rijeka, Croatia, 2012, pp. 191-210; R. Tamura, K. Suzuki, Y. Uchida, Y. Noda, *Electron Paramag. Reson.*, 2013, **23**, 1; R. Tamura, Y. Uchida, K. Suzuki, *Handbook of Liquid Crystals*, Second Edition, eds. J. W. Goodby, P. J. Collings, T. Kato, C. Tschierske, H. F. Gleeson, P. Raynes, Wiley-VCH, Weinheim, 2014, Vol. 8, pp. 837-864.

7 Y. Uchida, N. Ikuma, R. Tamura, S. Shimono, Y. Noda, J. Yamauchi, Y. Aoki, H. Nohira, *J. Mater. Chem.*, 2008, **18**, 2950; Y. Uchida, K. Suzuki, R. Tamura, N. Ikuma, S. Shimono, Y. Noda, J. Yamauchi, *J. Am. Chem. Soc.*, 2010, **132**, 9746.

8 K. Suzuki, Y. Uchida, R. Tamura, S. Shimono, J. Yamauchi, *J. Mater. Chem.*, 2012, **22**, 6799.

9 Y. Uchida, K. Suzuki, R. Tamura, *J. Phys. Chem. B*, 2012, **116**, 9791.

10 A. Kh. Vorobiev, N. A. Chumakova, D. A. Pomogailo, Y. Uchida, K. Suzuki, Y. Noda, *J. Phys. Chem. B*, 2014, **118**, 1932.

11 P. Ravat, T. Marszalek, W. Pisula, K. Müllen, M Baumgarten, *J. Am. Chem. Soc.*, 2014, **136**, 12860.

12 C. V. Yelamaggad, A. S. Achalkumar, D. S. S. Rao, M. Nobusawa, H. Akutsu, J. Yamada, S. Nakatsuji, *J. Mater. Chem.,* 2008, **18**, 3433.

13 S. Castellanos, F. López-Calahorra, E. Brillas, L. Juliá, D. Velasco, *Angew. Chem. Int. Ed.*, 2009, **48**, 6516.

14 A. Jankowiak, D. Pociecha, J. Szczytko, H. Monobe, P. Kaszyński, *J. Am. Chem. Soc.*, 2012, **134**, 2465.

15 I. Dierking, *Textures of Liquid Crystals*, Wiley-VCH, Weinheim, 2003.

16 V. A. Mallia, N. Tamaoki, *J. Mater. Chem.*, 2002, **13**, 219; C. Keith, A. Lehmann, U. Baumeister, M. Prehm, C. Tschierske, *Soft Matter*, 2010, **6**, 1704.

17 H. J. Müller, W. Haase, *J. Phys.* (*Paris*), 1983, **44**, 1209.

18 M. J. Frisch, G. W. Trucks, H. B. Schlegel, G. E. Scuseria, M. A. Robb, J. R. Cheeseman, G. Scalmani, V. Barone, B. Mennucci, G. A. Petersson, H. Nakatsuji, M. Caricato, X. Li, H. P. Hratchian, A. F. Izmaylov, J. Bloino, G. Zheng, J. L. Sonnenberg, M. Hada, M. Ehara, K. Toyota, R. Fukuda, J. Hasegawa, M. Ishida, T. Nakajima, Y. Honda, O. Kitao, H. Nakai, T. Vreven, J. A. Montgomery, Jr., J. E. Peralta, F. Ogliaro, M. Bearpark, J. J. Heyd, E. Brothers, K. N. Kudin, V. N. Staroverov, R. Kobayashi, J. Normand, K. Raghavachari, A. Rendell, J. C. Burant, S. S. Iyengar, J. Tomasi, M. Cossi, N. Rega, J. M. Millam, M. Klene, J. E. Knox, J. B. Cross, V. Bakken, C. Adamo, J. Jaramillo, R. Gomperts, R. E. Stratmann, O. Yazyev, A. J. Austin, R. Cammi, C. Pomelli, J. W. Ochterski, R. L. Martin, K. Morokuma, V. G. Zakrzewski, G. A. Voth, P. Salvador, J. J. Dannenberg, S. Dapprich, A. D. Daniels, Ö. Farkas, J. B. Foresman, J. V. Ortiz, J. Cioslowski, and D. J. Fox, GAUSSIAN 09, Revision D.01, Gaussian, Inc., Wallingford CT, 2009.

19 G. Pelzl, S. Diele, W. Weissflog, *Adv. Mater.*, 1999, **11**, 707; D. M. Walba, Top. *Stereochem*., 2003, **24**, 457; H. Takezoe, Y. Takanishi, *Jpn. J. App. Phys*., 2006, **45**, 597; R. Amaranatha, C. Tschierske, *J. Mater. Chem.,* 2006, **16**, 907; A. Eremin, A. Jákli, *Soft Matter*, 2013, **9**, 615.

20 K. Suzuki, Y. Uchida, R. Tamura, Y. Noda, N. Ikuma, S. Shimono. J. Yamauchi, *Soft Matter*, 2013, **9**, 4687; K. Suzuki, Y. Uchida, R. Tamura, Y. Noda, N. Ikuma, S. Shimono. J. Yamauchi, *Adv. Sci. Tech*., 2013, **82**, 50; R. Tamura, Y. Uchida, K. Suzuki, K. *Advances in Organic Crystal Chemistry: Comprehensive Reviews 2015*, eds. R. Tamura, M. Miyata, Springer, Tokyo, 2015, chap. 35, pp. 689-706.

21 Y. Uchida, Y. Iwai, T. Akita, T. Mitome, K. Suzuki, R. Tamura, N. Nishiyama, *J. Mater. Chem. B*, 2014, **2**, 4130.

22 C. Kumar, *Magnetic Nanomaterials*, Wiley-VCH, Weinheim, 2009; J. S. Wendelin, *Angew. Chem. Int. Ed.*, 2011, **50**, 1242.

23 J. B. Mitchell, S. Xavier, A. M. DeLuca, A. L. Sowers, J. A. Cook, M. C. Krishna, S. M. Hahn, A. Russo, *Free Radical Biol. Med.*, 2003, **34**, 93; D. Arieli, G. Nahmany, N. Casap, D. Ad-El, Y. Samuni, *Free Radical Res.*, 2008, **42**, 114; I. A. Grigor'ev, N. I. Tkacheva, S. V. Morozov, *Curr. Med. Chem.*, 2014, **21**, 2839.

ChemComm Accepted Manuscript